Virus Research 261 (2019) 65–71

Contents lists available at ScienceDirect

Virus Research

journal homepage: www.elsevier.com/locate/virusres

Dengue virus requires apoptosis linked gene-2-interacting protein X (ALIX) for viral propagation

Chutima Thepparit[a], Sarawut Khongwichit[a], Kunjimas Ketsuwan[a], Sirikwan Libsittikul[a], Prasert Auewarakul[b], Duncan R. Smith[a,*]

[a] Institute of Molecular Biosciences, Mahidol University, Salaya Campus, 25/25 Phuttamonthol Sai 4, Nakhon Pathom, Bangkok, 73170, Thailand
[b] Department of Microbiology, Faculty of Medicine, Siriraj Hospital, Mahidol University, 2 Prannok Rd, Bangkoknoi, Bangkok 10700, Thailand

ARTICLE INFO

Keywords:
Dengue virus
NS3
ALIX
AIP1
ESCRT
PDCD6IP

ABSTRACT

The endosomal sorting complexes required for transport (ESCRT) pathway accessory protein apoptosis linked gene-2-interacting protein X (ALIX) has been shown to be upregulated during dengue virus (DENV) replication. Yeast-two-hybrid screens have additionally shown that ALIX interacts with DENV NS3 protein, but evaluation of the interaction through a replicon assay failed to show a functional significance to the interaction. In this study the interaction between DENV NS3 and ALIX was investigated by co-immunoprecipitation, and functional significance assessed by investigation of DENV production in ALIX expression regulated cells. The results showed that ALIX both interacted and co-localized with DENV NS3 protein and that upregulation of ALIX resulted in a significantly increased viral titer, while either siRNA or CRISPR-Cas9 mediated down regulation of ALIX significantly reduced viral production, without affecting relative DENV genome levels. These results are consistent with ALIX playing a significant role in the DENV replication cycle either during late infection or at viral egress.

1. Introduction

Dengue is the most common arthropod-borne viral disease and is a significant public health problem in many countries. Approximately 390 million dengue infections are believed to occur annually across more than 100 countries worldwide and of these infections some 96 million result in some form of symptoms (Bhatt et al., 2013). The causative agent of dengue is the positive sense, single stranded RNA virus belonging to the family *Flaviviridae*, genus *Flavivirus*, species *Dengue virus*.

(DENV), which is comprised of four closely related but antigenically distinct viruses designated DENV 1 to DENV 4 (Gubler, 1998). The increasing distribution of the primary transmission agent of DENV *Aedes aegypti* and the secondary vector *Aedes albopictus* has driven much of the increase in dengue cases over the last 30 years (Jansen and Beebe, 2010; Lambrechts et al., 2010). This, coupled with increased global temperatures has led to the introduction of the disease to non-tropical countries as evidenced by the autochthonous outbreaks in Croatia (Gjenero-Margan et al., 2011) and metropolitan France (Marchand et al., 2013).

In humans, while infection with DENV can be asymptomatic, it frequently results in a relatively benign and self limiting febrile disease termed dengue fever although in a proportion of cases more serious consequences, characterized by hemorrhage and plasma leakage, can occur (Gubler, 1998). While the mechanism behind the more severe presentation remains to be fully elucidated, severe manifestation is often associated with a second infection with a heterologous DENV (Bravo et al., 1987). It is believed that while antibodies raised to a primary infection provide lifelong immunity to that virus, they offer only transient protection against a second infection with a heterologous infection. However, cross reactive but non-neutralizing antibodies can facilitate infection of Fcγ receptors (FcγR) bearing cells through internalization of a virus-antibody complex in the process known as antibody dependent enhancement (ADE) of infection (Halstead, 1989).

DENV enters non- FcγR bearing cells predominantly through a process of receptor mediated endocytosis (Cruz-Oliveira et al., 2015). After endosomal fusion and release of the nucleocapsid to the cytoplasm, the genomic RNA which is 5′-capped is translated directly into a single polypeptide encoding seven non-structural proteins (NS1, NS2A, NS2B, NS3, NS4A, NS4B, and NS5) and three structural proteins (capsid (C), pre-membrane (pr-M) and envelope (E)) that is processed by virally encoded and host cell proteases (Chang, 1997). The three structural proteins form the physical structure of the progeny virus, while the non-structural proteins play roles in regulating a variety of cellular

* Corresponding author.
E-mail addresses: duncan.smi@mahidol.ac.th, duncan_r_smith@hotmail.com (D.R. Smith).

https://doi.org/10.1016/j.virusres.2018.12.015
Received 12 May 2018; Received in revised form 4 December 2018; Accepted 28 December 2018
Available online 29 December 2018
0168-1702/

processes and form the replication complex which generates the progeny genomic RNA through a negative strand replicative intermediate molecule (Apte-Sengupta et al., 2014; Selisko et al., 2014).

The DENV NS3 protein is a multifunctional, multidomain protein with protease, helicase, and nucleoside 5′-triphosphatase (NTPase) activities (Bazan and Fletterick, 1989; Erbel et al., 2006; Meng et al., 2015; Xu et al., 2005). NS3 interacts with the virally encoded polymerase, DENV NS5 (Mackenzie, 2005), and with the cofactor required for protease activity, NS2B (Erbel et al., 2006) as well as with NS4B which promotes the helicase activity of NS3 (Umareddy et al., 2006). In addition to interactions with DENV encoded proteins, studies have shown that NS3 interacts with a number of host cellular proteins, including the nuclear receptor binding protein (NRBP) which influences cellular membrane alterations (Chua et al., 2004), fatty acid synthase which mediates alterations in lipid metabolism (Heaton et al., 2010) and ALIX (Apoptosis Linked gene-2-Interacting protein X) (Khadka et al., 2011), a protein also known as Program Cell Death 6 interacting Protein; PDCD6IP, AIP1). ALIX is an accessory protein in the endosomal sorting complexes required for transport (ESCRT) pathway (Bissig and Gruenberg, 2014), and it has been implicated in membrane acquisition for a number of viruses (Martin-Serrano et al., 2003). In addition to the interaction with DENV NS3 (Khadka et al., 2011) ALIX has been shown to interact with the NS3 protein of the closely related flavivirus Yellow fever virus (YFV) (Carpp et al., 2011). In YFV infection, ALIX has been shown to interact with a small tetrapeptide sequence “YPTI” (tyrosine, proline, threonine, and isoleucine) of NS3, and this interaction then recruits other ESCRT proteins to facilitate particle release (Carpp et al., 2011). DENV NS3 does not contain a YPTI motif, and while ALIX and DENV NS3 have been shown to interact in a high throughput yeast two hybrid system, knock down of ALIX had no effect on luciferase activity in a replicon system (Khadka et al., 2011). However, as noted by the authors, their assay did not evaluate all stages of the DENV replication cycle, and ALIX may therefore have an as yet unidentified role in the DENV replication cycle. Further evidence for a role for ALIX was provided by Pattanakitisakul and colleagues who showed that ALIX was up-regulated in the cytosol of DENV infected human endothelial cells (Pattanakitsakul et al., 2010). Given the contradictory evidence of the requirement for ALIX in dengue infection, this study aimed to shed more light on the involvement of cellular ALIX in the DENV replication cycle.

2. Material and methods

2.1. Cells, virus and transfection

HEK 293T/17 (human embryonic kidney) cells were grown and maintained in Dulbecco’s modified Eagle’s medium (DMEM, Gibco Invitrogen, Grand Island, NY) supplemented with 10% heat inactivated fetal bovine serum (FBS, Gibco Invitrogen), at 37 °C with 5% CO_2 (Heraeus Instrument; Langenselbold, Germany). Four DENV serotypes were used which are two laboratory adapted strains including DENV 2 (strain 16,681) and DENV 4 (strain 1036) and two clinical isolate strains DENV 1 (DENV-1/THAI/NS1-040/2006) and DENV 3 (DENV-3/THAI/NS1-007/2006) originally isolated from a dengue hemorrhagic fever patient and a dengue fever patient, respectively. All viruses were propagated and viral titers determined as described previously (Sithisarn et al., 2003). All infections were undertaken at a multiplicity of infection (MOI) of 5 and the percentage of infected cells was determined by flow cytometry exactly as described elsewhere (Panraksa et al., 2017). For transfection for immunofluorescence assays, HEK 293T/17 cells were preseeded on coverslips in 24 multi-well plate (4×10^5 cells/well) 1 day prior to transfection with mCherry-hALIX (a kind gift from James Hurley, Addgene plasmid#21504) or co transfection with mCherry-hALIX and a DENV 2 NS3 expressing construct using Lipofectamine LTX with Plus reagent (Invitrogen) according to the manufacturer’s protocol. Briefly, 0.8 µg of plasmids were incubated with Plus reagent in the presence of Opti-MEM serum free media prior to mixing with Lipofectamine LTX. The DNA-lipofectamine complex was added dropwise to cells and the transfected cells were incubated at 37 °C with 10% CO_2 for 6 h after which the media was replaced with fresh complete media. After 1 day post transfection, transfection efficiency was observed by detection of the mCherry expressing cells under a fluorescence microscope.

2.2. Co-immunoprecipitation (Co-IP)

Co-immunoprecipitation (Co-IP) assays were performed using Protein G Sepharose™ 4 Fast Flow (Amersham Bioscience, Piscataway NJ) according to the procedure described previously (Jirakanwisal et al., 2015) or using the Pierce Co-IP Kit (Thermo Fisher Scientific, Waltham MA, USA) according to the manufacturer’s protocol. Briefly, cell lysates were collected from non-infected and DENV infected HEK 293T/17 (MOI of 5) cells at 1 d.p.i. by lysis with IP Lysis/Wash Buffer (0.025 M Tris, 0.15 M NaCl, 0.001 M EDTA, 1% NP-40, 5% glycerol, pH 7.4). For each reaction, 1 mg of cell lysates were pre-cleared with 80 µl of the Control Agarose Resin slurry in a spin column in the presence of 1X coupling buffer at 4 °C for 1 h. After centrifugation, the flow-through pre-cleared lysates were collected for Co-IP assays. For antibody immobilization, 50 µl of the AminoLink Plus Coupling Resin was added into a Pierce spin column and washed with 1X coupling buffer. Then the resin was incubated with 10 µg of a mouse monoclonal antibody against ALIX (MA183977, Thermo Fisher Scientific) or quenching buffer as a negative control at room temperature for 2 h with gentle rotation. After washing the column several times with coupling buffer and wash buffer, the precleared cell lysates were added and samples were incubated in a rotator at 4 °C overnight. The IP reactions were then washed with IP Lysis/Wash buffer several times and eluted with elution buffer. The elution and flow-through fractions were collected and proteins were separated by SDS-PAGE before transfer to solid matrix support by electrotransfer. Membranes were probed with an anti-DENV NS3 antibody (PA5-32199, Thermo Fisher Scientific at a 1:1,000 dilution or GTX124252, GeneTex, Irvine CA at a 1:2,500 dilution) followed by incubation with a 1:6,000 dilution of a secondary mouse anti-rabbit antibody conjugated with HRP (Cat No.0747, Cell Signaling, Danvers, MA). Filters were stripped and re-probed with a 1: 1,000 dilution of a mouse monoclonal anti-ALIX antibody (MA1-83977, Thermo Fisher Scientific) followed by incubation with a secondary anti-mouse IgG antibody conjugated with HRP (A9044, Sigma-Aldrich Co., St. Louis, MO). Reverse Co-IP assays were performed by pulling down DENV NS3 from infected cell lysates with an anti-DENV NS3 antibody (GTX124252, GeneTex) and probing the filter with a mouse monoclonal anti-ALIX antibody (MA1-83977, Thermo Fisher Scientific).

2.3. Immunofluorescence assay

Cells grown on glass coverslips were fixed with 4% paraformaldehyde for 15 min prior to permeabilized with 0.5% Triton X-100 in PBS for 10 min. Cells were incubated with a 1:100 dilution of a mouse monoclonal antibody against DENV E protein (MA1-27093, Thermo Fisher Scientific) or a1:500 dilution of a rabbit polyclonal antibody against DENV NS3 (PA5-32199, Thermo Fisher Scientific) for 2 h in humidified chamber, followed by incubation with a 1:200 dilution of a FITC conjugated anti-mouse IgG antibody (KPL, Gaithersburg, MD) or a 1:200 dilution of a FITC conjugated anti-rabbit IgG antibody (Santa Cruz Biotechnology, Inc., Santa Cruz, CA), respectively. The cells were then counterstained with 0.5 µg/ml DAPI prior to mounting with ProLong Gold Antifade reagent (Thermo Fisher Scientific). Slides were examined using a confocal laser scanning microscope (FV10i, Olympus). For colocalization analysis, Pearson’s correlation coefficients were determined from 12 fields of each group using the Image J program (Abramoff et al., 2004) with the JACoP plugin (French et al., 2008) as described previously (Panyasrivanit et al., 2009).

2.4. siRNA construction

siRNAs targeted to human ALIX were constructed using the Silencer® siRNA Construction Kit (Thermo Fisher Scientific). siRNA target sites were designed based on the complete sequence of the human ALIX mRNA sequence (*Homo sapiens* programmed cell death 6 interacting protein, mRNA (cDNA clone MGC:87040 IMAGE:4830724), complete cds (GenBank accession number BC068454.1). Sequences of 21 nt in length starting with an AA dinucleotide were selected and analyzed to check cross specificity with other coding sequences. Five sequences with 30–50% GC content that are specific to ALIX located at different positions along the full-length of the ALIX sequence were chosen as the siRNA target sites. To construct the siRNAs, sense and antisense templates were generated based on the selected target sequences with an additional T7 promoter primer (5'-CCTGTCTC-3') at the 3'end (Supplementary Table 1). siRNA templates and primers used in this study were synthesized by Macrogen company (Seoul, Korea). An additionl siRNA specific to green fluorescent protein (GFP: GenBank accession number U50974) was additionally constructed. The sequences were subjected to siRNA template construction using the Ambion Silencer siRNA Construction kit (Thermo Fisher Scientific) according to the manufacturer's protocols.

2.5. siRNA transfection

HEK 293T/17 cells were reverse-transfected with or without siRNAs using Lipofectamine RNAiMAX (Life Technologies, Grand Island, NY). A total of 250 pmol siRNAs were incubated with 1.5 µL of Lipofectamine RNAiMAX diluted in 50 µL Opti-MEM (Life Technologies) for 20 min in a well of a 24 multi-well plate. Then 4×10^5 HEK 293T/17 cells in DMEM with 10% FBS were seeded in each well and cultured at 37 °C in humidified incubator with 5% CO_2. Each transfection was performed in duplicate. The transfected cells were collected for 5 days post transfection and total RNAs were isolated using Tri reagent (Sigma-Aldrich, St. Louis, MO) to examine the mRNA expression level of ALIX by Real-Time PCR.

2.6. CRISPR-Cas9 mediated ALIX knock-down in HEK2 93T/17 cells

An alternative CRISPR-Cas9 approach was performed to knock-down endogenous ALIX expression in HEK 293T/17 cells. The plasmid expressing the Cas9 system from *Streptococcus pyogenes* with 2A-Puro and cloning backbone for guide RNA, pSpCas9(BB)-2A-Puro (PX459) V2.0 was a gift from Feng Zhang (Addgene plasmid #62988 ; http://n2t.net/addgene:62988; RRID:Addgene_62988) (Ran et al., 2013). The 20-nt single guide RNA (sgRNA) sequence targeting ALIX DNA sequence directly upstream of a 5'-NGG PAM site was selected from exon 1 of the ALIX genomic DNA sequence on human chromosome 3 using the guide RNA selection tool CRISPOR (http://crispor.tefor.net/crispor.py). The sgRNA with its antisense sequence (Supplemental Table 2) were phosphorylated and annealed prior to cloning into the plasmid at the *Bpi*I restriction site and the constructs were validated by nucleotide sequencing. One µg of the control pSpCas9(BB) plasmid or the pSpCas9(ALIX) plasmid containing sgRNA targeting ALIX DNA were transfected into 1×10^5 HEK 293T/17 cells. After 24 h post transfection, cells bearing plasmids were then selected with 2 µg/ml of puromycin. The expression of ALIX was determined by western blot analysis using a 1:1,000 dilution of anti-ALIX antibody (ab88388; Abcam, Cambridge, UK) and re-probed with a 1:150 dilution of GAPDH antibody (DSHB-hGAPDH-2G7; obtained from the Developmental Studies Hybridoma Bank, created by the NICHD of the NIH and maintained at The University of Iowa, Department of Biology, Iowa City, Iowa.)

2.7. Reverse transcription and real-time PCR

Total RNAs extracted from the collected cells were treated with DNaseI prior to converting to cDNA using ImProm-II™ reverse transcriptase (Promega, Madison, WI). One µg of DNaseI-treated RNAs diluted in nuclease free distilled water were mixed with 0.5 µg of random hexamer in a total 5 µL reaction prior to heating at 70 °C for 5 min and immediate chilling on ice. Reverse transcription was achieved using ImProm-II reverse transcriptase in 1X ImProm-II™ buffer with 1.5 mM $MgCl_2$ and 0.5 mM each dNTP at 25 °C for 5 min followed by incubation at 42 °C for 60 min prior to heating at 70 °C for 15 min. One µL of cDNA was then used directly in the Real-Time PCR reaction. Twenty µL of Real-Time PCR reaction composing of 1X KAPA SYBR FAST qPCR kit (KAPA Biosystems, Wilmington, MA), 1 µL of cDNA and 200 µM of each primer. For each reaction, the expression of actin was determined for normalization. All primer sequences are given in Supplemental Table 3. The real-time PCR reaction was performed in a Mastercycler ep realplex (Eppendorf, Hamburg, Germany) using the following conditions: initial denaturation at 95 °C for 3 min followed by 40 cycles of 95 °C for 1 min, 55 °C for 30 s, 72 °C for 20 s and melting curve analysis by heating at 95 °C for 15 s, 60 °C for 15 s and heating up to 95 °C for 15 s. Threshold cycles (CT) for amplification of ALIX and actin genes from each reaction were determined and the relative expression of ALIX was analyzed using 2-ΔΔ CT algorithm. ΔCT is the relative expression of ALIX to actin mRNA (ΔCT = CT ALIX- CT Actin) and ΔΔCT is the relative ALIX expression of the treated group normalized with the control group (ΔΔCT = ΔCT siALIX- ΔCT siGFP). For relative DENV genome quantification, ΔCT was determined (ΔCT = CT NS1- CT Actin).

2.8. Statistical analysis

Statistical analysis of significance between datasets was undertaken by one-way ANOVA followed by post test, Tukey's multiple comparison using the GraphPad Prism software version 5.00 (GraphPad Software, Inc). A P-value ≤ 0.05 was taken as a significant difference.

3. Results

3.1. DENV NS3 protein interacts with ALIX

Given that YFV NS3 has been shown to interact with ALIX we initially determined whether there was an interaction between DENV NS3 and ALIX, despite DENV 2 NS3 not having the YPTI motif implicated in the YFV NS3: ALIX interaction (Carpp et al., 2011). ALIX was therefore pulled down from uninfected and DENV 2 infected cell lysates, and the immunoprecipitation complexes probed for the presence of NS3 by western blotting. Results (Fig. 1) showed that NS3 was coimmunoprecipitated with ALIX, and the IP control without antibody showed that the precipitation of ALIX was specific. The specific interaction of DENV NS3 and ALIX was confirmed by co-IP and reverse co-IP using other DENV serotypes including a laboratory-adapted DENV 4 and low passage clinical isolates of DENV 1 and DENV 3. The results showed the interaction of ALIX with NS3 of DENV 2, 3, and 4, but not DENV 1 (Supplementary Fig. 1). However the percentage infection of DENV 1 was comparatively low (approximately 20%) and this may have affected the result (Supplementary Fig. 2). In all cases, a lower level of precipitated ALIX was seen in the uninfected cells as compared to the DENV infected cells. While it is possible that this arises from ALIX being increased in DENV infection as has been reported by some authors (Pattanakitsakul et al., 2010), in our hands western analysis of ALIX in DENV infection failed to show a statistically significant increase in ALIX expression (Supplementary Fig. 3), suggesting that other factors are mediating the lower levels of precipitated ALIX in uninfected cells.

3.2. Colocalization of DENV NS3 and ALIX

Given the demonstrated interaction between DENV NS3 and ALIX, we next sought to determine whether there was cellular colocalization of these two proteins. HEK 293T/17 cells were transfected with

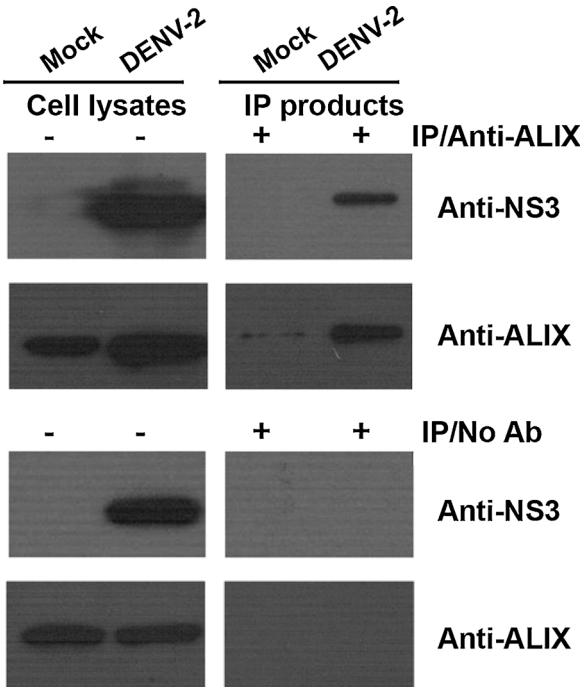

Fig. 1. Interaction between ALIX and DENV-2 NS3.
DENV-2 infected or mock infected cell lysates were subjected to immunoprecipitation with an antibody directed against ALIX or without antibody. The IP products were subjected to Western blot analysis using an antibody against DENV NS3. The membrane was re-probed with antibody against ALIX to confirm the pull down reaction.

mCherry-hALIX and subsequently infected with DENV-2. On day 1 post infection, the cells were fixed and immunostained for either DENV NS3 or DENV E protein using appropriate antibodies. The images were assessed under a confocal microscope and the degree of colocalization was determined based on Pearson's correlation coefficients using the Image *J* program (Abramoff et al., 2004) with the JACoP plugin (French et al., 2008) as described previously (Panyasrivanit et al., 2009). Results (Fig. 2A and B) showed that there was a marked difference in the degrees of colocalization between ALIX and DENV NS3 (Pearson's correlation coefficients = 0.490 ± 0.026) and ALIX and DENV E protein (Pearson's correlation coefficients = 0.014 ± 0.017).

To confirm the colocalization between ALIX and DENV NS3, HEK 293T/17 cells were cotransfected with mCherry-hALIX and a DENV-NS3 expressing plasmid and the degree of colocalization again confirmed by confocal imaging and evaluation of Pearson's correlation coefficient. The results (Fig. 2C) showed clear colocalization between the two proteins, with a Pearson's correlation coefficient (0.493 ± 0.035) highly similar to that determined with DENV infection of cells transfected with mCherry-hALIX. The results are consistent with a specific interaction and colocalization between DENV NS3 and ALIX.

3.3. The role of ALIX in DENV infection

To determine whether the interaction between DENV NS3 and ALIX was functionally relevant to the DENV replication cycle, HEK 293T/17 cells were transfected with mCherry-hALIX and the control mCherry plasmid prior to infection with DENV 2. The overexpression of ALIX in mCherry-hALIX but not mCherry control plasmids transfected cells was observed as the additional upper band by western blotting analysis (Supplementary Fig. 3). At 2 days post infection virus titer in the supernatant was determined by standard plaque assay. The results showed a significant increase of viral titer in the cells transfected with mCherry-hALIX comparatively to the control cells and the control plasmid transfected cells (Fig. 3).

3.4. ALIX is involved in DENV production but not in viral RNA replication

To further explore the functionality of the ALIX NS3 interaction, the expression of ALIX was down regulated by RNA interference using siRNAs prior to infection with DENV 2. HEK 293T/17 cells were transfected with 5 different siRNAs targeted to human ALIX (si-hALIX1, 2, 3, 4, and 5) and a control anti-GFP siRNA. The mRNA expression of ALIX in the treated cells was investigated daily for 5 days post-transfection by real-time PCR with normalization against actin. The results showed that all of the siRNAs were able to reduce expression of ALIX on day 3 post-transfection (Fig. 4A), while no significant reduction in ALIX expression was seen with transfection with the siRNA targeted to GFP. The greatest reduction in expression was observed with si-hALIX2 whose effect on ALIX expression was additionally observed for 5 days

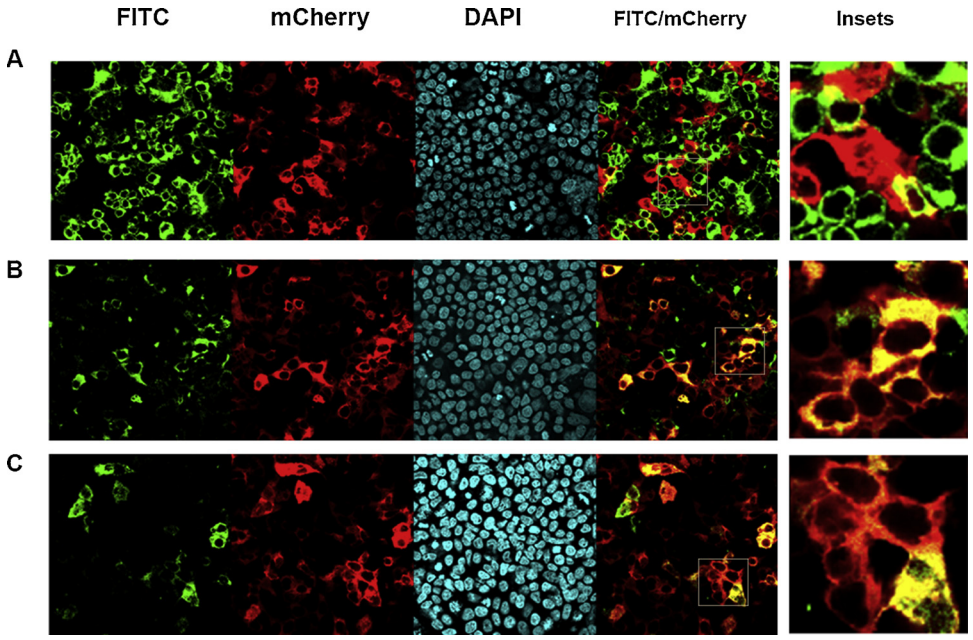

Fig. 2. Colocalization between ALIX and DENV NS3 after infection.
HEK 293T/17 cells expressing mCherry-hALIX were infected with DENV-2 and subsequently examined for the localization of DENV-2 E protein (green, A) or DENV-2 NS3 (green, B) with mCherry-hALIX (red), or doubly transfected with plasmid containing DENV-2 NS3 (green, C).
Nuclei were additionally stained with DAPI (blue). Fluorescent signals were observed under an Olympus FV10i confocal microscope. Enlarged inserts are also shown.

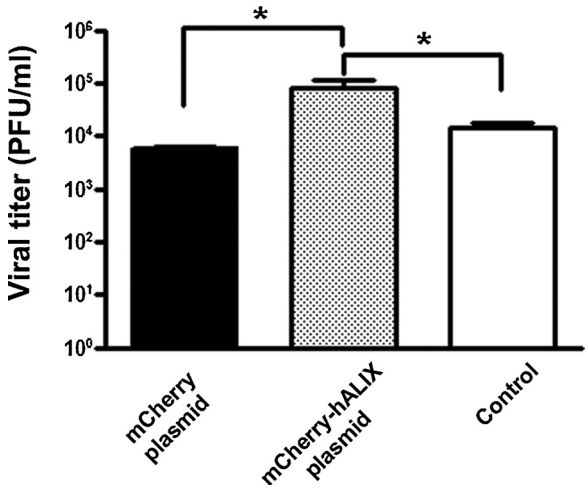

Fig. 3. Role of ALIX in DENV infection.
HEK 293T/17 cells expressing mCherry-hALIX were infected with DENV-2 and the titer of DENV was determined by standard plaque assay. Experiments were undertaken independently in triplicate, with virus titer determined in duplicate. Asterisks represent a significant difference, P-value ≤ 0.05.

post-transfection (Supplementary Fig. 4), while si-hALIX4 showed the least efficiency in reducing ALIX expression.

To observe the effect on the DENV replication cycle of a reduction in ALIX expression, cells were again treated with the 5 siRNAs and subsequently infected with DENV 2 on day 3 post transfection. At 24 hs post infection virus titer in the supernatant was determined by standard plaque assay, while the level of ALIX expression was determined by real-time PCR. Results (Fig. 4A) showed that although ALIX expression was not completely down-regulated, significant reductions in virus titer were seen with 4 of the 5 siRNAs targeted to ALIX, and that the reductions in titer were broadly consistent with the reductions seen in ALIX expression. In addition the relative DENV genome level was established by real-time PCR for si-hALIX 2 and 3, the siRNAs showing the largest decrease in ALIX expression and virus titer, and in parallel with the siRNA targeting to GFP. Results (Fig. 4B) showed that no significant differences were seen in relative genome copy number between the siRNAs targeting ALIX and the control infection with the siRNA targeted to GFP. These results were confirmed in the ALIX knock-out HEK 293T/17 cells mediated by CRISPR-Cas9 system (Fig. 4C and D) which supported that the absence of ALIX expression did not impact DENV replication but only on viral production.

4. Discussion

The involvement of host cell ALIX during DENV infection has been previously documented. Pattanakitsakul and colleagues investigated proteomic changes in different cellular compartments of human endothelial cells upon DENV-2 infection and reported the up-regulation of two isoforms of ALIX in the cytosolic fraction (Pattanakitsakul et al., 2010). In the study the authors reported the colocalization of ALIX with late endosomal lysobisphosphatidic acid (LBPA), a marker of the late endosome where DENV membrane fusion occurs after endocytosis (van der Schaar et al., 2007; Zaitseva et al., 2010). Pretreatment of cells with an antibody directed against LBPA delayed DENV E protein synthesis and reduced viral production, from which the authors proposed a role for an ALIX-LBPA interaction in DENV protein synthesis and replication (Pattanakitsakul et al., 2010). The direct interaction between DENV NS3 and ALIX was established by a high-throughput yeast two-hybrid screen for DENV interacting proteins (Khadka et al., 2011) although interestingly a similar methodology screening for flavivirus (dengue, Japanese encephalitis, tick-borne encephalitis, and West Nile viruses) NS3 and NS5 interacting proteins failed to detect the interaction between ALIX and NS3 (Le Breton et al., 2011). Interestingly, although Khadka and colleagues observed the interaction between DENV NS3 and ALIX in their screen, they showed that down-expression of cellular ALIX in the liver cell line used had no effect on DENV replication in a replicon assay system (Khadka et al., 2011). Our study confirmed this observation that ALIX down regulation did not affect DENV replication *per se*, but assay of virus titer showed a large effect on virus production that was broadly consistent with the degree of ALIX down-regulation, suggesting the involvement of ALIX at a late stage of viral production or at viral egress.

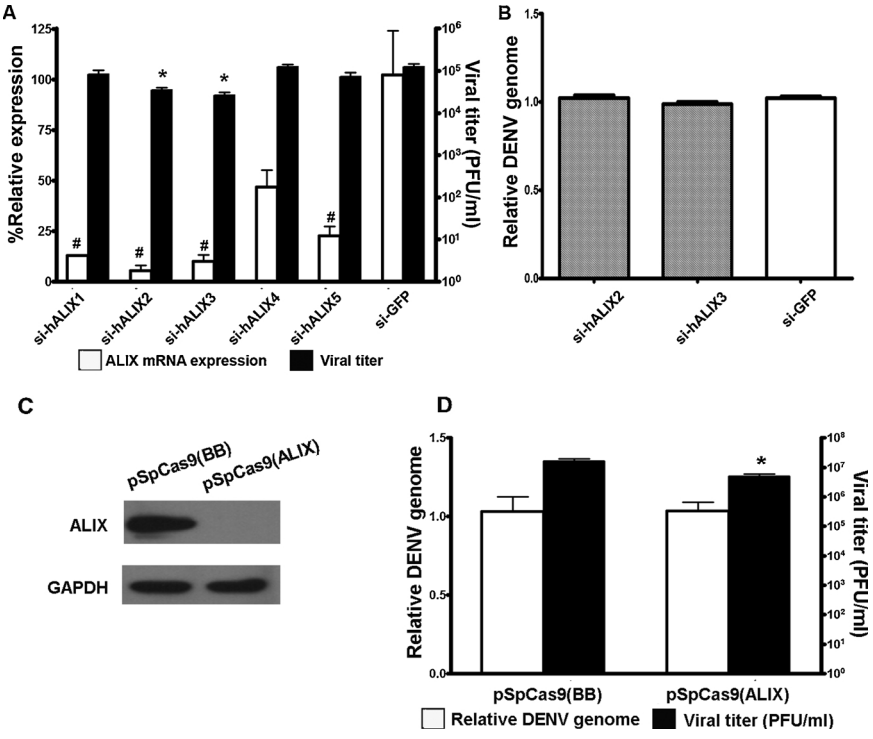

Fig. 4. ALIX is involved in DENV production but not in viral RNA replication.
Expression of ALIX was down regulated through transfection with siRNAs before infection with DENV-2. At 3 days post transfection (A) the relative expression of ALIX was determined by quantitative PCR and is shown after normalization with actin and displayed relative to siGFP as 100% (white bars, left Y axis) and the titer of DENV determined by standard plaque assay (filled bars, right Y axis) and (B) for selected siRNA transfections the relative level of DENV genome determined by quantitative PCR. si-GFP is a non-relevant siRNA and control is non-transfected, DENV infected cells. (C) Western blot analysis of the expression of ALIX to GAPDH of the control pSpCas9(BB) or pSpCas9(ALIX) transfected HEK 293T/17 cells. (D) The relative level of DENV genome (white bars, left Y axis) and the titer of DENV (filled bars, right Y axis) of the DENV-infected control and CRISPR-Cas9 ALIX knock-down HEK 293T/17 cells. Experiments were undertaken independently in triplicate, with virus titer determined in duplicate. Hashtags represent the significant difference from the ALIX mRNA expression level of the siGFP transfected control. Asterisks represent a significant difference from the viral titer of the siGFP transfected control, P-value ≤ 0.05.

ALIX is a multifunctional protein in the ESCRT pathway which was initially identified as trafficking machinery for delivery of multivesicular bodies for degradation within vacuoles or lysosomes of mammalian cells (Henne et al., 2011; Schmidt and Teis, 2012). The ESCRT machinery comprises five distinct ESCRTs complexes (ESCRT-0, -I, -II, -III and the Vps4 complexes) and several accessory proteins (Henne et al., 2011; Schmidt and Teis, 2012). ALIX is an accessory protein interacting with components of both ESCRT-I and ESCRT-III (Martin-Serrano et al., 2003) and the ESCRT machinery has been implicated in viral budding for several enveloped viruses including several flaviviruses (Carpp et al., 2011; Dilley et al., 2010; Ku et al., 2014; Tabata et al., 2016; Votteler and Sundquist, 2013). Specifically ESCRT machinery was found to be essential for the formation of viral particles or the release of viruses but not viral replication in flavivirus including the hepatitis C virus, JEV and DENV (Corless et al., 2010; Tabata et al., 2016). Tabata and colleagues showed that the flavivirus budding process involving specific ESCRT factors starting with the recruitment of TSG101 to the budding site on the ER membrane resulting in downstream recruitment of charged MVB proteins, CHMP4 and CHMP2/3. Subsequently CHMP4 forms the circular filaments inside the neck-like structure and the CHMP2/3 family caps the filaments inducing membrane fission (Tabata et al., 2016). Although ALIX was not reported as the ESCRT factor in the virus budding model mentioned earlier, the involvement of ALIX in virus releasing was demonstrated in YFV (Carpp et al., 2011).

Enveloped viruses recruit ESCRT pathway proteins through three classes of short consensus peptides termed late domains which include PT/SAP, PPXY, and LYPXnL (P; proline, T; threonine, S; serine, A; alanine, L; leucine, X; any residue and n; 1–3 residues). The LYPXnL motifs have been shown to mediate retroviral budding by binding to ALIX (Dilley et al., 2010; Votteler and Sundquist, 2013). For YFV, ALIX mediates the release of infectious YFV particles via the interaction with NS3 protein through a small tetrapeptide sequence “YPTI” and ALIX then recruits other ESCRT proteins to facilitate particle release (Carpp et al., 2011). Although a late domain in DENV NS3 protein has not been identified, at the same position as the YFV NS3 late domain all 4 serotypes of DENV share a similar ‘YXKT’ motif.

The tyrosine residue of the late domain was found to be the most critical residue affecting ALIX binding affinity and specificity (Zhai et al., 2008), The ALIX V domain, a topological complex of 11 alpha-helices forming a V-shape was structurally identified as the hydrophobic binding pocket of the YPXnL late domain (Lee et al., 2007) and the tyrosine residue of the late-domain has the most distinctive interaction with ALIX by binding deep in the ALIX V binding domain, forming hydrogen-bond interactions with conserved residues in the center of ALIX V pocket. Substitution of tyrosine in the late-domain of HIV-1 p6Gag and EIAV p9Gag with phenylalanine reduced the binding affinity of both proteins more than 15-fold (Zhai et al., 2008). This suggests that the interaction between DENV NS3 and ALIX might occur through the late domain-like motif through the high affinity N’ terminal tyrosine residue. It also suggests that disruption of this interaction may form the basis of a specific anti-DENV therapy by inhibiting viral release, and thus reducing viral spread and viremia.

5. Conclusion

Our results show that ALIX interacts with DENV NS3 of both laboratory adapted and clinical isolate strains. The upregulation of ALIX resulted in a significantly increased viral titer, whereas ALIX down regulation mediated by siRNA or CRISPR-Cas9 significantly reduced viral production, without affecting relative DENV genome levels. These results are consistent with ALIX playing a significant role in the DENV replication cycle either during late infection or at viral egress.

Declarations of interest

None.

Acknowledgements

This work was supported by Mahidol University, the Thailand Research Fund (IRN60W0002) and Mahidol University and the Thailand Research Fund (BRG6080006). We are thankful to Dr. Nawapol Kunkeaw who provided expertise in the CRISPR-Cas9 experiment and Ms. Potchaman Sittipaisankul for confocal technical support.

Appendix A. Supplementary data

Supplementary material related to this article can be found, in the online version, at doi:https://doi.org/10.1016/j.virusres.2018.12.015.

References

Abramoff, M.D., Magelhaes, P.J., Ram, S.J., 2004. Image processing with ImageJ. Biophotonics Int. 11 (7), 36–42.
Apte-Sengupta, S., Sirohi, D., Kuhn, R.J., 2014. Coupling of replication and assembly in flaviviruses. Curr. Opin. Virol. 9, 134–142.
Bazan, J.F., Fletterick, R.J., 1989. Detection of a trypsin-like serine protease domain in flaviviruses and pestiviruses. Virology 171 (2), 637–639.
Bhatt, S., Gething, P.W., Brady, O.J., Messina, J.P., Farlow, A.W., Moyes, C.L., Drake, J.M., Brownstein, J.S., Hoen, A.G., Sankoh, O., 2013. The global distribution and burden of dengue. Nature 496 (7446), 504–507.
Bissig, C., Gruenberg, J., 2014. ALIX and the multivesicular endosome: ALIX in Wonderland. Trends Cell Biol. 24 (1), 19–25.
Bravo, J.R., Guzman, M.G., Kouri, G.P., 1987. Why dengue haemorrhagic fever in Cuba? 1. Individual risk factors for dengue haemorrhagic fever/dengue shock syndrome (DHF/DSS). Trans. R. Soc. Trop. Med. Hyg. 81 (5), 816–820.
Carpp, L.N., Galler, R., Bonaldo, M.C., 2011. Interaction between the yellow fever virus nonstructural protein NS3 and the host protein Alix contributes to the release of infectious particles. Microbes. Infect. 13 (1), 85–95.
Chang, G.J., 1997. Molecular biology of dengue viruses. In: Gubler, D.J., Kuno, G. (Eds.), Dengue and Dengue Hemorrhagic Fever. CAB International, Wallingford, pp. 175–198.
Chua, J.J., Ng, M.M., Chow, V.T., 2004. The non-structural 3 (NS3) protein of dengue virus type 2 interacts with human nuclear receptor binding protein and is associated with alterations in membrane structure. Virus Res. 102 (2), 151–163.
Corless, L., Crump, C.M., Griffin, S.D., Harris, M., 2010. Vps4 and the ESCRT-III complex are required for the release of infectious hepatitis C virus particles. J. Gen. Virol. 91 (Pt 2), 362–372.
Cruz-Oliveira, C., Freire, J.M., Conceicao, T.M., Higa, L.M., Castanho, M.A., Da Poian, A.T., 2015. Receptors and routes of dengue virus entry into the host cells. FEMS Microbiol. Rev. 39 (2), 155–170.
Dilley, K.A., Gregory, D., Johnson, M.C., Vogt, V.M., 2010. An LYPSL late domain in the gag protein contributes to the efficient release and replication of Rous sarcoma virus. J. Virol. 84 (13), 6276–6287.
Erbel, P., Schiering, N., D’Arcy, A., Renatus, M., Kroemer, M., Lim, S.P., Yin, Z., Keller, T.H., Vasudevan, S.G., Hommel, U., 2006. Structural basis for the activation of flaviviral NS3 proteases from dengue and West Nile virus. Nat. Struct. Mol. Biol. 13 (4), 372–373.
French, A.P., Mills, S., Swarup, R., Bennett, M.J., Pridmore, T.P., 2008. Colocalization of fluorescent markers in confocal microscope images of plant cells. Nat. Protoc. 3 (4), 619–628.
Gjenero-Margan, I., Aleraj, B., Krajcar, D., Lesnikar, V., Klobucar, A., Pem-Novosel, I., Kurecic-Filipovic, S., Komparak, S., Martic, R., Duricic, S., Betica-Radic, L., Okmadzic, J., Vilibic-Cavlek, T., Babic-Erceg, A., Turkovic, B., Avsic-Zupanc, T., Radic, I., Ljubic, M., Sarac, K., Benic, N., Mlinaric-Galinovic, G., 2011. Autochthonous dengue fever in Croatia, August-September 2010. Euro Surveill. 16 (9), 19805.
Gubler, D.J., 1998. Dengue and dengue hemorrhagic fever. Clin. Microbiol. Rev. 11 (3), 480–496.
Halstead, S.B., 1989. Antibody, macrophages, dengue virus infection, shock, and hemorrhage: a pathogenetic cascade. Rev. Infect. Dis. 11 (Suppl. 4), S830–839.
Heaton, N.S., Perera, R., Berger, K.L., Khadka, S., Lacount, D.J., Kuhn, R.J., Randall, G., 2010. Dengue virus nonstructural protein 3 redistributes fatty acid synthase to sites of viral replication and increases cellular fatty acid synthesis. Proc. Natl. Acad. Sci. U. S. A. 107 (40), 17345–17350.
Henne, W.M., Buchkovich, N.J., Emr, S.D., 2011. The ESCRT pathway. Dev. Cell 21 (1), 77–91.
Jansen, C.C., Beebe, N.W., 2010. The dengue vector Aedes aegypti: what comes next. Microbes Infect. 12 (4), 272–279.
Jirakanwisal, K., Srisutthisamphan, K., Thepparit, C., Suptawiwat, O., Auewarakul, P., Paemanee, A., Roytrakul, S., Smith, D.R., 2015. Identification of Hsp90 as a species independent H5N1 avian influenza A virus PB2 interacting protein. Comp. Immunol.

Microbiol. Infect. Dis. 43, 28–35.
Khadka, S., Vangeloff, A.D., Zhang, C., Siddavatam, P., Heaton, N.S., Wang, L., Sengupta, R., Sahasrabudhe, S., Randall, G., Gribskov, M., Kuhn, R.J., Perera, R., LaCount, D.J., 2011. A physical interaction network of dengue virus and human proteins. Mol. Cell Proteomics 10 (12) M111 012187.
Ku, P.I., Bendjennat, M., Ballew, J., Landesman, M.B., Saffarian, S., 2014. ALIX is recruited temporarily into HIV-1 budding sites at the end of gag assembly. PLoS One 9 (5), e96950.
Lambrechts, L., Scott, T.W., Gubler, D.J., 2010. Consequences of the expanding global distribution of Aedes albopictus for dengue virus transmission. PLoS Negl. Trop. Dis. 4 (5), e646.
Le Breton, M., Meyniel-Schicklin, L., Deloire, A., Coutard, B., Canard, B., de Lamballerie, X., Andre, P., Rabourdin-Combe, C., Lotteau, V., Davoust, N., 2011. Flavivirus NS3 and NS5 proteins interaction network: a high-throughput yeast two-hybrid screen. BMC Microbiol. 11, 234.
Lee, S., Joshi, A., Nagashima, K., Freed, E.O., Hurley, J.H., 2007. Structural basis for viral late-domain binding to Alix. Nat. Struct. Mol. Biol. 14 (3), 194–199.
Mackenzie, J., 2005. Wrapping things up about virus RNA replication. Traffic 6 (11), 967–977.
Marchand, E., Prat, C., Jeannin, C., Lafont, E., Bergmann, T., Flusin, O., Rizzi, J., Roux, N., Busso, V., Deniau, J., Noel, H., Vaillant, V., Leparc-Goffart, I., Six, C., Paty, M.C., 2013. Autochthonous case of dengue in France, October 2013. Euro Surveill. 18 (50), 20661.
Martin-Serrano, J., Yarovoy, A., Perez-Caballero, D., Bieniasz, P.D., 2003. Divergent retroviral late-budding domains recruit vacuolar protein sorting factors by using alternative adaptor proteins. Proc. Natl. Acad. Sci. U. S. A. 100 (21), 12414–12419.
Meng, F., Badierah, R.A., Almehdar, H.A., Redwan, E.M., Kurgan, L., Uversky, V.N., 2015. Unstructural biology of the dengue virus proteins. FEBS J. 282 (17), 3368–3394.
Panraksa, P., Ramphan, S., Khongwichit, S., Smith, D.R., 2017. Activity of andrographolide against dengue virus. Antiviral Res. 139, 69–78.
Panyasrivanit, M., Khakpoor, A., Wikan, N., Smith, D.R., 2009. Co-localization of constituents of the dengue virus translation and replication machinery with amphisomes. J. Gen. Virol. 90 (Pt 2), 448–456.
Pattanakitsakul, S.N., Poungsawai, J., Kanlaya, R., Sinchaikul, S., Chen, S.T., Thongboonkerd, V., 2010. Association of Alix with late endosomal lysobisphosphatidic acid is important for dengue virus infection in human endothelial cells. J. Proteome Res. 9 (9), 4640–4648.
Ran, F.A., Hsu, P.D., Wright, J., Agarwala, V., Scott, D.A., Zhang, F., 2013. Genome engineering using the CRISPR-Cas9 system. Nat. Protoc. 8 (11), 2281–2308.
Schmidt, O., Teis, D., 2012. The ESCRT machinery. Curr. Biol. 22 (4), R116–120.
Selisko, B., Wang, C., Harris, E., Canard, B., 2014. Regulation of Flavivirus RNA synthesis and replication. Curr. Opin. Virol. 9, 74–83.
Sithisarn, P., Suksanpaisan, L., Thepparit, C., Smith, D.R., 2003. Behavior of the dengue virus in solution. J. Med. Virol. 71 (4), 532–539.
Tabata, K., Arimoto, M., Arakawa, M., Nara, A., Saito, K., Omori, H., Arai, A., Ishikawa, T., Konishi, E., Suzuki, R., Matsuura, Y., Morita, E., 2016. Unique requirement for ESCRT factors in Flavivirus particle formation on the endoplasmic reticulum. Cell Rep. 16 (9), 2339–2347.
Umareddy, I., Chao, A., Sampath, A., Gu, F., Vasudevan, S.G., 2006. Dengue virus NS4B interacts with NS3 and dissociates it from single-stranded RNA. J. Gen. Virol. 87 (Pt 9), 2605–2614.
van der Schaar, H.M., Rust, M.J., Waarts, B.L., van der Ende-Metselaar, H., Kuhn, R.J., Wilschut, J., Zhuang, X., Smit, J.M., 2007. Characterization of the early events in dengue virus cell entry by biochemical assays and single-virus tracking. J. Virol. 81 (21), 12019–12028.
Votteler, J., Sundquist, W.I., 2013. Virus budding and the ESCRT pathway. Cell Host Microbe 14 (3), 232–241.
Xu, T., Sampath, A., Chao, A., Wen, D., Nanao, M., Chene, P., Vasudevan, S.G., Lescar, J., 2005. Structure of the Dengue virus helicase/nucleoside triphosphatase catalytic domain at a resolution of 2.4 A. J. Virol. 79 (16), 10278–10288.
Zaitseva, E., Yang, S.T., Melikov, K., Pourmal, S., Chernomordik, L.V., 2010. Dengue virus ensures its fusion in late endosomes using compartment-specific lipids. PLoS Pathog. 6 (10), e1001131.
Zhai, Q., Fisher, R.D., Chung, H.Y., Myszka, D.G., Sundquist, W.I., Hill, C.P., 2008. Structural and functional studies of ALIX interactions with YPX(n)L late domains of HIV-1 and EIAV. Nat. Struct. Mol. Biol. 15 (1), 43–49.